JPE 18-4-22

https://doi.org/10.6113/JPE.2018.18.4.1201
ISSN(Print): 1598-2092 / ISSN(Online): 2093-4718

Practical Implementation of Maximum Power Tracking Based Short-Current Pulse Method for Thermoelectric Generators Systems

Khalid Yahya†, Mehmet Zeki Bilgin*, and Tarik Erfidan*

†,*Department of Electrical Engineering, Kocaeli University, Kocaeli, Turkey

Abstract

The applications of thermoelectric generators (TEGs) have received a lot of attention both in terms of harvesting waste thermal energy and the need for multi-levels of power. It is critical to track the optimum electrical operating point using DC to DC converters controlled by a pulse that is generated through a maximum power point tracking algorithm (MPPT). In this paper, the hardware implementation of a short-current pulse algorithm has been demonstrated under steady stated and transient conditions. In addition, the MPPT algorithm has been proposed, which is one of the most effective and applicable algorithms for obtaining the maximum power point of TEGs. During this study, the proposed prototype has been validated both analytically and experimentally. It has also demonstrated successful performance, which highlights the claimed advantages of the proposed MPPT solution.

Key words: Boost converter, Maximum power point tracking (MPPT), Short-current pulse (SCP), Thermoelectric generator (TEG)

I. INTRODUCTION

Maximizing electrical energy generation through renewable energy sources aims to get rid of conventional sources and to generate electric energy with the lowest losses, lowest noise, lowest pollution, longest life, etc. Thermoelectric power generation (TEG) is a promising source due to the mentioned operational advantages. A TEG device can convert heat energy directly into electric energy (seebeck effect) without the need for fuel consumption. The phenomenon of power generation is made possible by exploiting a temperature gradient between two surfaces of a thermal electric device.

Because of the operational conditions surrounding the TEG and its manufactured nature that enables it to work under different conditions, there are some unhandled factors that prevent developers from extracting the maximum power of a TEG system. One of these essential factors is temperature mismatching, which can be considered as wasted energy. Whenever there is a transient in the temperature difference, the internal resistance of the TEG is changed, which hampers the system to be operated at the optimum operation point [1]. Due to dynamic conditions, it is necessary to develop special maximum power point tracking (MPPT) schemes that can track the real maximum power point (MPP) under mismatch conditions taking into account the tracking time for reduced losses and a high-performance system.

The DC-DC converter is the heart of MPPT, which used as an interface between the renewable source and the load by adjusting the duty ratio of the converter untill the MPP can be achieved. TEG devices have been employed in different applications for electronic devices as mentioned in [2]. Later, they started to be used in medical applications [3]. Recently the authors of [4] attempted to apply TEGs for improving water heater efficiency. Nowadays, they are being used for applying a large scale of ten heat pumps that increases power plant efficiency and there is a bundle of studies [5]-[7] that sheds light on different TEG applications in multi-disciplines such as solar thermoelectric generators (STEGs), automobiles, combined heat and power (CHP) systems, etc.

Huge industries such as steel-making, glass-making, and cement production are consuming a great deal of energy in the form of heat. Operating a TEG in similar atmospheres is

Manuscript received Oct. 29, 2017; accepted Feb. 13, 2018
Recommended for publication by Associate Editor Jonghoon Kim.
†Corresponding Author: khalid.omy@gmail.com
Tel: +90-507-1406936, Kocaeli University
*Department of Electrical Engineering, Kocaeli University, Turkey

suitable and highly recommended since this environment assists the TEG to obtain the optimal benefits of this wasted energy. On the other hand, several researchers have studied the concept of ocean thermal energy conversion (OTEC) as a large-scale TEG application and stated that it is essential for the TEG to have a larger figure of merit for high conversion efficiency [8]. Additionally, large-scale applications have expanded to have certain considerations towards the effect of the heat distribution of the hot and cold side, which leads to power mismatch loss, and the necessity to characterize the TEG array for implementing an effective MPPT to handle this mismatch.

Several tests to characterize the TEG were proposed in [9]-[12] and they have accurate characteristic results. In this study, the characters of three commercial TEG have been elicited by a simple test under steady state and dynamic conditions. Furthermore, several MPPT algorithms were used to track the MPP for photovoltaic systems and adjusted to be applied to TEGs. Perturb and Observe (P&O) [13]-[17] is widely used in tracking the MPP because of its ability to achieve the optimum point. However, P&O has some drawbacks, such as the value of oscillations around the MPP being contingent upon the step size of the duty cycle, having a small step size to ensure small oscillations with a slow climbing to the MPP and a big step size to drawn big oscillations with fast climbing. Another algorithm called incremental conductance (IC) [18] has been convoluted and its exactitude depends on the iteration size. Because of the linearity of the TEG characteristics, the fractional open circuit voltage and fractional short-circuit-current [19]-[21] are highly recommended. These algorithms work with one sensor so that the optimum operation point of the TEG can be obtained based on open circuit-voltage (V_{oc}) or short circuit current (I_{sc}). However, the estimation of V_{oc}/I_{sc} is not valid in real applications because the internal resistance is changing based on the change of the temperature difference. The authors of [21] proposed a technique to perform the open-circuit voltage measure during pseudo normal operation without any disconnecting from the load side.

In this paper, a simple test was done for characterizing TEG and extracting the optimum value of the MPP under different conditions. Then a boost converter was designed to interface the TEG with the load. Moreover, a short-current pulse (SCP) MPPT algorithm was implemented by using a short-current pulse circuit and a single current sensor. Fig. 1 shows a general schematic of the proposed harvesting system. This method can effectively track the maximum optimal point without measuring the output power of the TEG.

The organization of this paper is as follows. Section II discusses the thermoelectric power generator device characteristics. Section III describes the test configuration and presentes the output characteristics of TEG in the dynamic state, outlining their operation as well as their advantages and disadvantages. Section IV looks at how the short-current pulse MPPT Algorithm was modified for the proposed harvesting system and gives a glimpse of the mechanism of the algorithm. Section V presents some experimental results and describes the implementation steps of the experiment and the SCP algorithm. Section VI contains some experimental results as well as a discussion of the factors that caused them. Section VII focus on the impact from the economic perspective. Finally, Section VIII provides the conclusion.

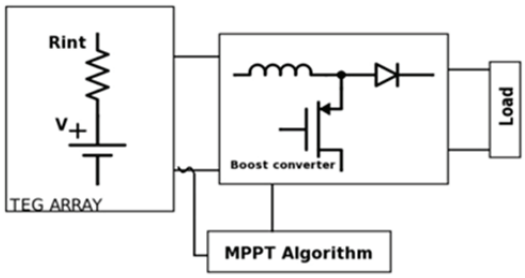

Fig. 1. Schematic of the proposed harvesting system.

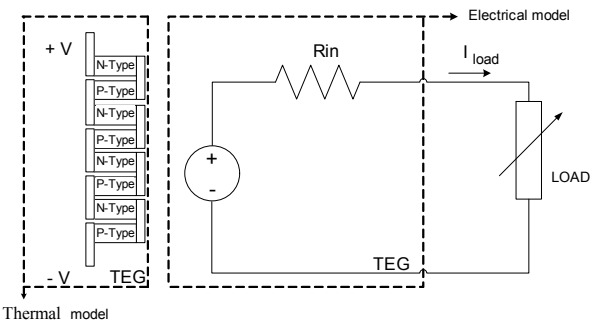

Fig. 2. Electrical and thermal model of a thermoelectric generator.

II. Thermoelectric Power Generator Device Characteristics

Fig. 2 illustrates the electrical and thermal structure of the TEG model. Previously, the TEG devices utilized two metallic materials, whereas recently manufactured TEGs use two different materials with alternating n-type and p-type semiconductor materials. The TEG structure is a "sandwich model", where the semiconductor materials are sandwiched between two ceramic plates for uniform thermal expansion. One of the two ceramic plates has a high temperature. As a result, it is called the hot side of the TEG. Meanwhile the other side has a low temperature and is called the cold side of the TEG. Between the TEG material and the metal heat exchangers electrical insulate thermal conductive layers usually exist. The ends of the n-type and p-type semiconductors are linked together by using metal junctions, which is commonly defined as thermocouple [7].

The thermal-electrical conversion is done by a phenomenon generally referred to as the "Seebeck Effect." When there is a temperature difference applied on the p-n type thermocouples,

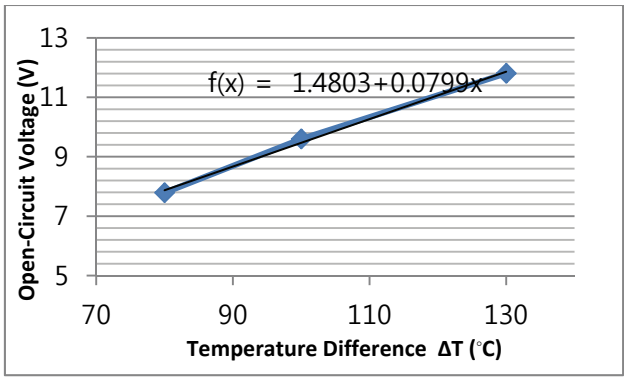

Fig. 3. Open-circuit voltage versus the temperature difference of a TEG.

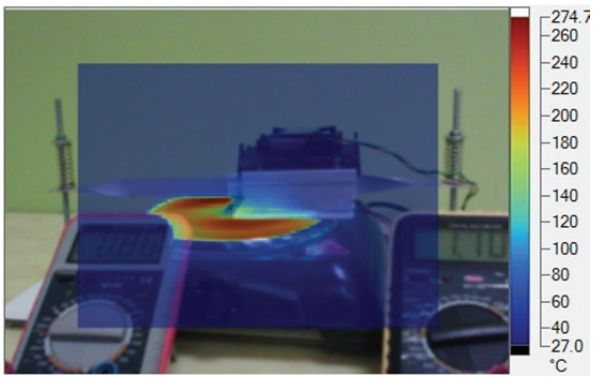

Fig. 4. The experimental test for a TEG.

a potential voltage is generated among the terminals of the circuit, which is known as the Seebeck effect. Descriptively, TEGs are considered as solid state device operated under steady and dynamic states with move-less parts along with features that enable them to produce no noise and involve no harmful agents. A TEG can be designed by a voltage source electrically linked in series with a resistance [21]. From the equivalent circuit of the TEG, the voltage and power are calculated as a function of the current load and temperature differences. In the steady state, it can be written that it changed imperceptibly with a temperature difference and it affects the characteristics of the TEG.

The magnitude of the open circuit voltage (V_{OC}) is linearly dependent on the temperature difference ΔT and the Seebeck coefficient (α) (V_{OC} = α ΔT) with respect to the TEG materials. For the high performance of TEG devices, the materials should have the following features:

- Large Seebeck Coefficients (α).
- High Electrical Conductivity (σ).
- Low Thermal Conductivity (K).

These features are set together and called the figure-of-merit (ZT) as shown in Equ. (1).

$$ZT = \left(\frac{\alpha 2\sigma}{K}\right) T \quad (1)$$

When the TEG is operating in the steady state, the output voltage can be represented as a straight line function f(x)=b+ax, where f(x) is the electric voltage, x is the temperature difference (ΔT) across the TEG surface and a,b are the constant numbers and can be experimentally calculated using the Gaussian elimination method from the variation of open circuit voltage with ΔT as shown in Fig. 3.

III. Test Configuration

The prototype in this paper is designed to study TEG performance, to provide accurate repeatable measurements and to get the TEG electrical characteristics. The TEG device is sandwiched between a hot block and a cold block. The experiment contains a high-temperature block heated by an electric stove, whilst the cold block is cooled by a heat sink connected to a fan unit. The output of the TEG is connected to a variable resistive load. The commercial TEG (TEP1-142T300) used in this paper was characterized by three different temperature gradients ΔT: 80 ˚C, 100 ˚C and 130 ˚C.

Fig. 4 shows the test platform and it provides real measurements under temperature differences across the TEG terminal with various resistive loads.

As a result of the platform test, the principle of the TEG is operating based on the applied temperature difference, which causes a potential energy to appear on the terminals. This energy relies on the conversion efficiency of the TEG, which is a significant matter for recovering the waste heat energy to electrical energy in all real applications such as automobiles, medical, solar thermoelectric generators, etc. The efficiency of a TEG device (η_{TEG}) is the ratio of the generated electrical power (P_{TEG}) by the TEG and the thermal energy. Fig. 5 shows the TEG power generation performance under different thermal energies.

$$\eta_{TEG} = \frac{P_{TEG}}{Q_H} \quad (2)$$

Where Q_H, the thermal energy rate applied to the hot surface, is given by:

$$Q_H = \frac{\Delta T}{Q_m} + \alpha\, T_H I_{TEG} - \frac{1}{2}\, R_{int} I_{TEG}^2 \quad (3)$$

Where Q_m is the thermal resistance of the TEG, T_H is the hot surface temperature, I_{TEG} is the generated current and R_{int} is the internal resistance of the TEG module. From Equs. (2) and (3) the efficiency of the selected module at different ΔT is shown in the Fig. 6.

Whenever a variation of ΔT appeared on the TEG materials, an immediate change occurs in the electrical characteristics of the TEG i.e. a change in the open circuit voltage, short circuit current and absolute value of R_{int} that depends on the temperature at which the TEG is operating. Hence, the optimum power does not have a fixed value, whereas the optimum operating power can be achieved when the current/voltage = $I_{SC}/2$ or $V_{OC}/2$. Due to the instability of the temperature gradient, the maximum power operating point would be changed as shown in Fig. 7.

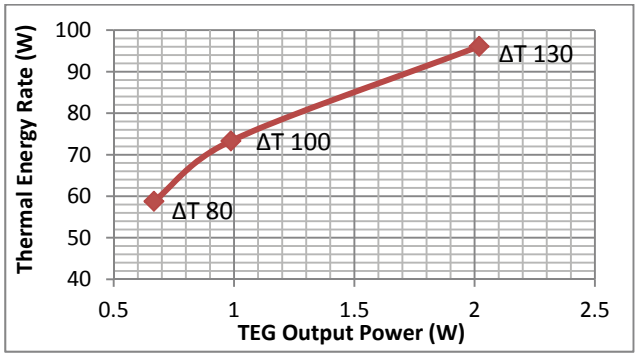

Fig. 5. Thermal energy vs. TEG output power under various ΔT.

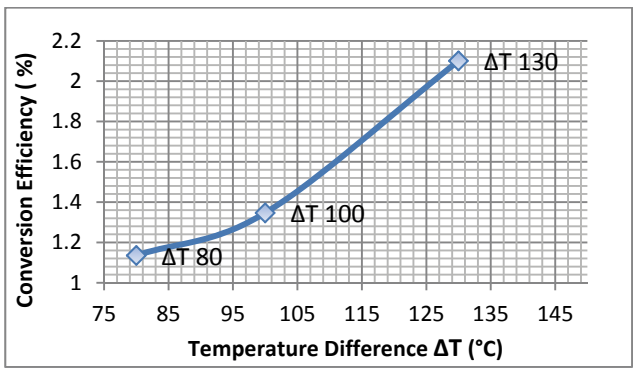

Fig. 6. Conversion efficiency of the TEG under various ΔT.

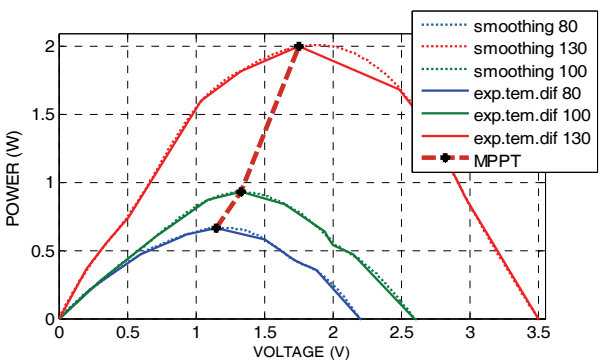

Fig. 7. P-I Characterization of a TEG Mode (TEP1-142T300).

For the employed TEG module, the maximum power point of three different ΔT and changes of the internal resistance of the TEG are shown in Table I. On the other hand, Fig. 8 shows the changes of the out power according to the changes of ΔT. In Fig. 8 (a) the red curve illustrates an increment of the temperature on the hot side of the TEG while the blue curve shows the cold side temperature and the incensement of ΔT under dynamic states at 4 ohm. Fig. 8 (b) clarifies the relation between the TEG output power and the temperature difference ΔT with respect to the TEG material.

The harvesting energy of TEG systems relies on the value of the internal resistance of the TEG and the load impedance. Naturally, the internal resistance changes with an alteration of the temperature difference across the thermocouples.

As a result of dynamic conditions, in order to harvest the

TABLE I
PERFORMANCE PARAMETERS OF A TEG

ΔT(°C)	V(V)	I(A)	MPP(W)	R_{int}(ohm)
80	1,15	0,58	0,667	2,206897
100	1,41	0,7	0,987	2,314286
130	1,96	1,03	2,0188	2,951456

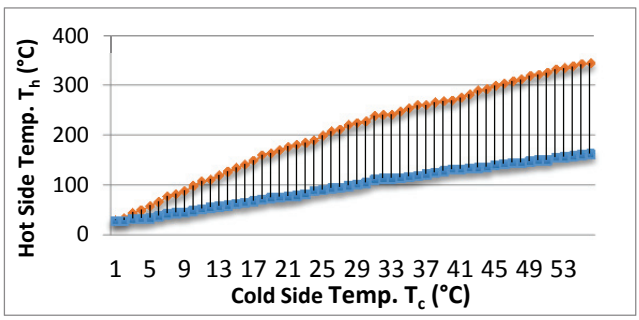

(a)

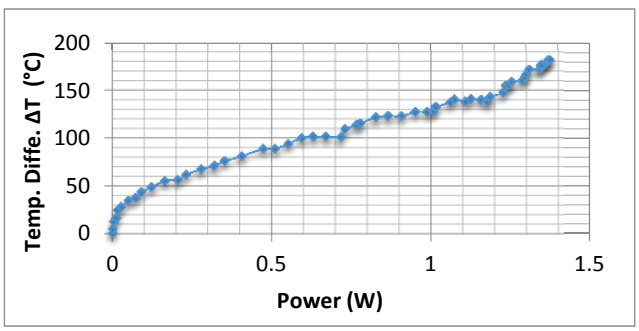

(b)

Fig. 8. Graphs showing: (a) Increment of the temperature difference on the TEG surfaces; (b) Relation between the TEG output power and the temperature difference ΔT.

maximum energy from the TEG systems and to minimize the cost produced power, it is necessary to develop a special maximum power point tracking (MPPT) algorithm that is able to matches and interface the load sink (R_L), which is run by the TEG model to its absolute internal resistance through modifying the duty cycle (D) of the converter. The internal resistance can be expressed as shown in Equ. (4). It is also used to verify the algorithm, which can track the real maximum power point (MPP) under mismatch factors.

$$R_{int} \approx (1 - D^2) + R_L \quad (4)$$

IV. MPPT CONVERTER

The core of MPPT hardware is a switch-mode DC-DC converter. It is widely used in DC power supplies and DC motor drives for the purpose of converting unregulated DC input into a controlled DC output at a desired voltage level. MPPT uses the same converter for various purposes: regulating the input voltage at the PV MPP and for providing load matching for the maximum power transfer.

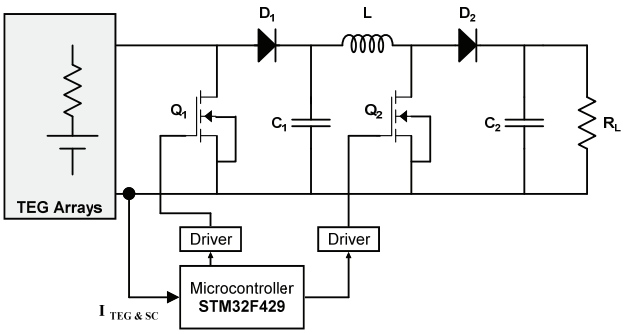

Fig. 9. Schematic diagram for the required components of the proposed technique.

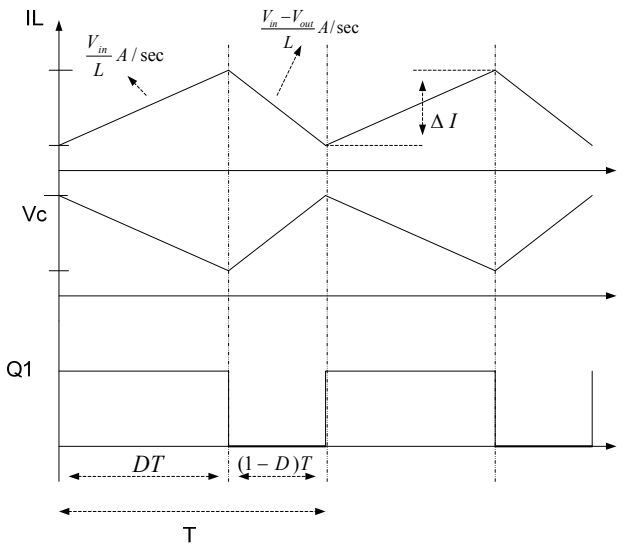

Fig. 10. Inductance current, capacitor voltage and gate signal in the CCM.

The generated energy from the TEG module is very low. There are some steps that can be followed to maximize the output power; making a TEG-array with n TEG modules and using a boost converter, which boosts the input voltage with respect to the circuit design. In this study, the configuration of the MPPT system built in laboratory is composed of a TEG array (three TEG modules connected in series), a short-current pulse circuit, and a boost converter controlled by the proposed MPPT, which is linked to a resistive load. A schematic diagram of the proposed system is shown in Fig. 9.

In order to measure the short circuit current of the proposed system, a Short-Current Pulse (SCP) technique has been proposed and implemented as shown in Fig. 9. The SCP circuit consists of a MOSFET, a Shockley diode (SK0726) and a capacitor. The MOSFET is connected in parallel with the TEG, the Shockley diode is linked to the MOSFET and the capacitor connected in parallel. The MOSFET is used to have a short circuit periodically between the TEG terminals derived by (TLP350). The diode is used to avoid the discharge of the input capacitor through the MOSFET during the on-time of the switching period. The capacitor is

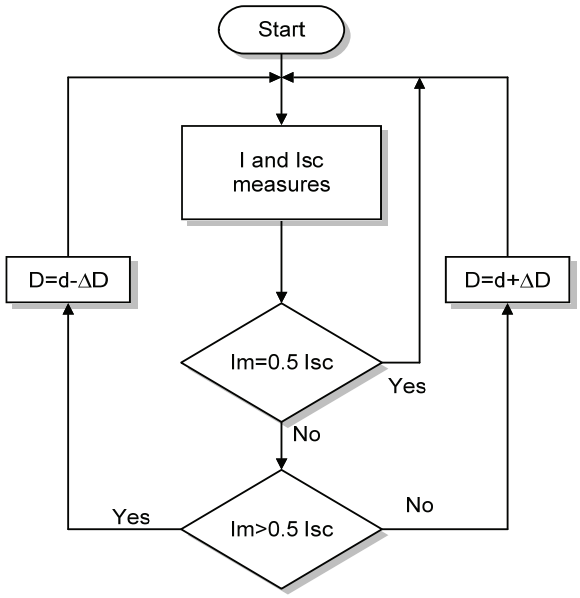

Fig. 11. Flow chart of the SCP algorithm.

implemented to supply the system during the on-time period and to guaranty that there is no loss of power drawn on the load. The voltage rating of the capacitor should have the same range as the open voltage circuit.

For the boost converter during the on-time, the switch Q_2 is closed (on-time) and no current passes through the diode D_2. The stored energy in the output capacitor C_2 supplies the load, while the circuit in the open circuit position crosses the diode D_2, and the output power of the TEG in this switching period is stored by the input capacitor and inductor. During the off period of the switch Q_2, the current does not pass through the switch. Instead, it passes through the diode D_2. The stored energy from the on-time period in the inductor along with the energy generated from the TEG flows towards the load. Fig. 10 shows the inductance current and the capacitor voltage with a gate signal in the continuous conduction mode (CCM). Regarding the above mentioned steps, it is observed that the output voltage is higher than the input voltage.

V. Short-Current Pulse MPPT Algorithm

The principle of the Short-Current Pulse (SCP) algorithm depends on a natural relationship between the optimum current I_m (the current at the maximum power point) and the short-circuit current I_{SC}, as mentioned in section III, which is based on the Equ. (5), where the algorithm has been built.

$$I_m = 0.5\, I_{sc} \tag{5}$$

The mechanism of the Short-Current Pulse algorithm, as shown in Fig. 11, is measuring and comparing both the current and the short circuit current. If the measured current is greater than half of the short circuit current, it means that the operating point of the TEG is on the left side of the maximum optimum power point. In another case, if the current

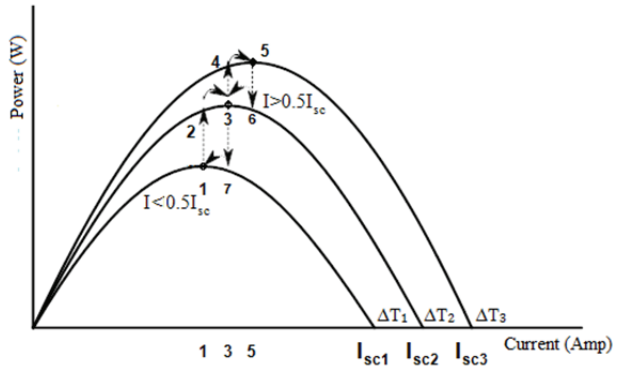

Fig. 12. Mechanism of the short-current pulse algorithm.

is smaller than half of the short circuit current, the operating point of the TEG is on the right side of the maximum optimum power point. Based on this, the MPP location has been confirmed and tracked by a given small step move to achieve the MPP. This operation is done periodically to grab the MPP in the steady and dynamic states.

The above steps are further explained in Fig. 12. It is presumed that; position 1 on the power current curve shows the initial optimum power point of the first temperature difference (ΔT_1). According to Equ. (6), the output power is affected due to the temperature difference ΔT.

$$P_L = \left(\frac{\alpha^2 \Delta T^2}{(R_{int}+R_L)^2}\right) R_L \quad (6)$$

Where, P_L is the power drawn on the load, α is the Seebeck coefficient, R_{int} is the internal resistance, and R_L is the load resistance.

Due to the temperature difference increment to ΔT_2, the operational point transfers from position 1 to position 2. Additionally, measuring the current with the short circuit current and comparing them with each other can enable the MPP to reach position 3 in the pre-designed steps. If the temperature difference rises to ΔT_3, the operating point approaches position 4. The regular measurement of both the current and the short circuit current determine the MPP position with the given steps and reaches position 5. On the other hand, if the reverse situation occurs due to a decrease in the temperature difference from ΔT_3 to ΔT_1, following the same stated steps would enable the algorithm to successfully obtain the MPP from 5 to 1 under different conditions.

VI. Experimental Results And Discussion

This paper presented the implementation of harvesting energy systems in the laboratory and proposed a short circuit current technique for a MPPT algorithm to track the optimum maximum power of three series 44x44mm commercial TEG modules. Fig. 13 shows the experiment elements of the proposed harvesting system circuit.

The hardware of the proposed harvesting system has low-cost high-performance elements. A high sensitivity INA250

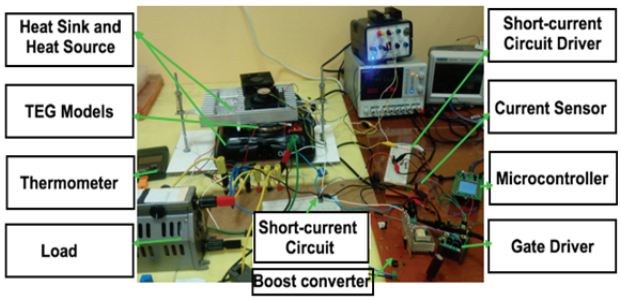

Fig. 13. Proposed harvesting system.

TABLE II
Results of the SCP Algorithm

ΔT(°C)	V(V)	MPP(W)	V_{MPPT}(V)	P_{MPPT} (W)
80	1,15	0,667	1,13	0,664
100	1,41	0,987	1,41	0,986
130	1,96	2,0188	1,96	2,011

is used for sensing the current. A STM32f429 discovery kit with ARM® Cortex®-M4 core is used. This kit equipped with a screen that gives the ability to verify whether the implemented algorithm it is operating properly or not. It also has the ability to present the measured parameters such as the short circuit current, the output current of the TEG, the duty steps and the operating duty cycle of the boost converter at the MPP. For this experiment, to match the turn on voltage (the output voltage capability of the microcontroller) of the chosen MOSFET, two gate drivers have been built to drive the MOSFET of the SCP and to boost converter circuit. The proposed prototype implementation is shown in Fig. 13.

The proposed algorithm is able to harvest the maximum energy, and it has been tested under two operating conditions, the steady state operating condition for three different temperature gradients ΔT_1=80 °C, ΔT_2=100 °C and ΔT_3= 130 °C; and the transit operating condition while the temperature has a range from (80°C to 130°C). Furthermore, the boost converter is designed in the continuous conduction mode to meet the maximum power point according to the transient range. For the transient case, the magnitude of the duty cycle was calculated dependent on the open circuit voltage of the TEG between V_{oc} 80°C = 7.79V and V_{oc} 130°C = 11.81V, since the output voltage of the TEG is equal to half of V_{oc} in Equ. (7) and Fig. 14. The calculated duty cycle ratio is further used to select the inductor, which guaranties that the boost converter operates in the CCM.

$$D_{CCM\Delta T} = \left(1 - \frac{V_{OC/2}}{V_{out}}\right) \quad (7)$$

$$D_{CCM80} = \left(1 - \frac{3.895}{15}\right) = 0.74033$$

$$D_{CCM130} = \left(1 - \frac{5.905}{15}\right) = 0.60633$$

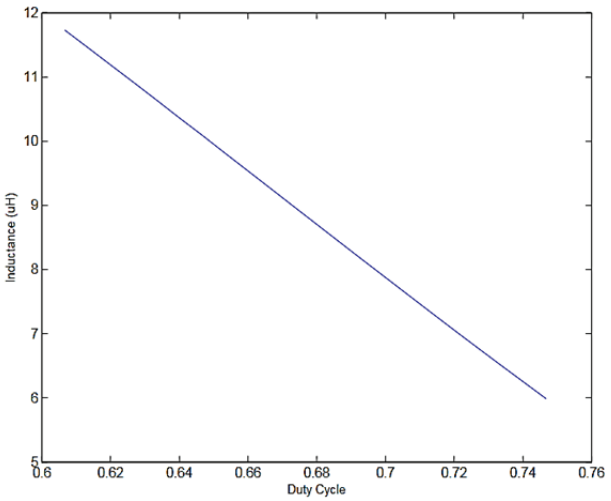

Fig. 14. Inductor selection for a boost converter.

As can be seen in Fig. 15, the TEG takes a long time to achieve stability when compared to the response time of the boost converter. The SCP algorithm has a high tracking performance and the average tracking efficiency is close to 100%, where the short-circuit current is measured three times per second to adjust the operating point and the controlled through pulse generated by the maximum power point tracking algorithm.

Moreover, there is an ability to increase and decrease the short-circuit current pulses per second by changing the sampling value in the code, which is implemented in the STM32f429.

For high-efficiency harvesting systems it is necessary to extract the optimum power from the TEG arrays under different temperature gradients. As mentioned in section II, three different ΔTs were applied on the TEG module and shown at three different operation points. Table II presents the results under the steady-state conditions. The P_{MPPT} column shows the optimum power extracted from the TEG under three different ΔTs, which shows the tracking accuracy of the proposed algorithm.

During transient operation, the temperature differences across the TEG are continuously changing, which affects the characteristics of the device. In this paper, the algorithm was tested under thermal transient conditions from 80˚C to 130˚C and the adjustment of the operation point was fitting three times per second through the duty cycle of the boost converter. Fig. 16 shows the voltage variation at the transient condition from 1.15V to 2V. The results of the experiment showed successful tracking of the optimum power point.

Based on the measured output power (P_{TEG_MPP}) of the TEG at the optimum point and the measured power with the use of the SCP MPPT algorithm (P_{TEG_MPPT}) under various temperature differences, the efficiency reached 99.89 %. Fig. 17 shows the efficiency of the algorithm, which is calculated by the following formula:

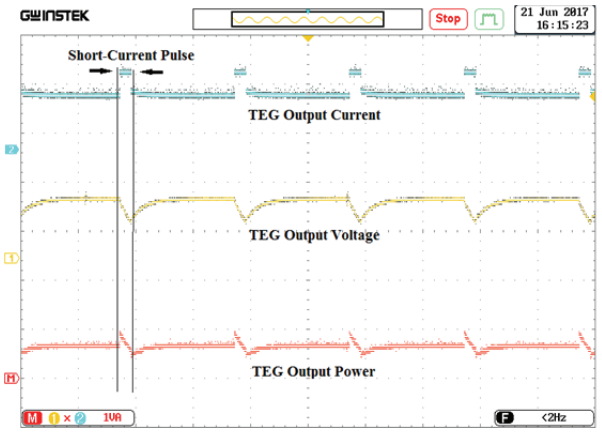

Fig. 15. Output power, current and voltage of three series TEP1-142T300 with a STM32F429 microcontroller.

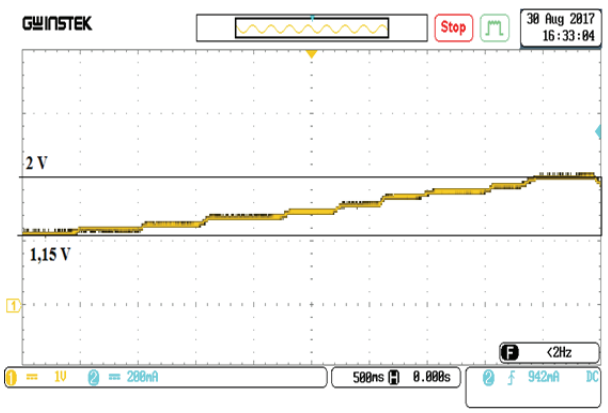

Fig. 16. Response of the SCP MPPT algorithm under transient conditions (1,15v to 2v) due to a change of ΔT (80 ◦C to 130◦C).

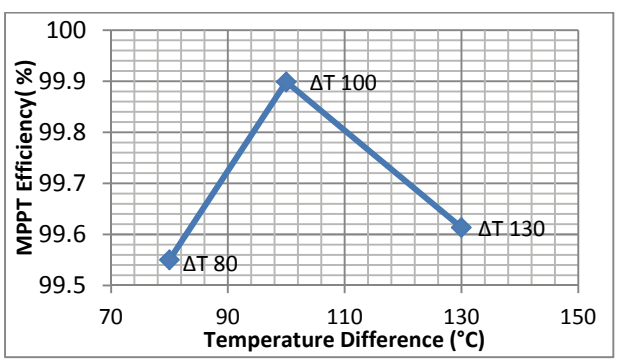

Fig. 17. Efficiency of the SCP MPPT algorithm under various temperature differences.

$$\eta_{MPPT} = \frac{P_{TEG\_MPPT}}{P_{TEG\_MPP}} * 10 \quad (8)$$

TEGs are good conversion devices that provide a few watts for multidisciplinary applications. Furthermore, the low efficiency of the TEG is not an obstacle as long as the contribution of the TEG gets benefits from the waste heat. Additionally, well-designed energy harvesting applications are able to take on a vital role in defeating the low-efficiency

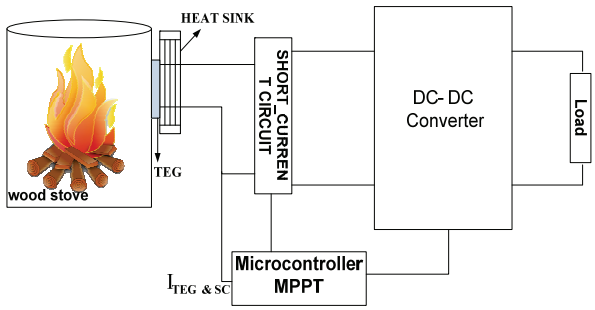

Fig. 18. TEG application scheme for the wood stove.

of TEGs and guaranteeing high-performing applications with the advantages of improved economics and preserving natural resources.

One of the most popular applications used in recovering waste heat energy is called the "wood stove". Electrically, the TEG application efficiency can be effectively increased through direct implementation of a MPPT algorithm to extract the maximum power which also decreases the cost of the output energy. Fig. 18 illustrates a reliable design for TEG applications with simple and low-cost features. Furthermore, there are certain calculations that have to be applied in order to get the aimed design. These calculations are used as a reference help to analyze both the rate of the input thermal energy rate Q_H as shown in Equ. (3) and the heat removal rate of the cold side Q_c from the following equation:

$$Q_c = \frac{\Delta T}{Q_m} + \alpha\, T_C I_{TEG} + \frac{1}{2}\, R_{int} I_{TEG}^2 \quad (9)$$

Based on the measured temperature difference, the TEG current can be calculated as follows:

$$I_{TEG} = \frac{\alpha\,(T_H - T_C)}{R_{int} + R_L} \quad (10)$$

The voltage at the maximum power is given by:

$$V_{TEG} = \frac{n\alpha\,(T_H - T_C)}{R_{int} + R_L} \quad (11)$$

Where n is the number of the thermocouples in the TEG module. With regard to developing areas and compose zones where there is no electricity access, the wood stove may provide approximately 35 kWh of energy by consuming around 10 KG of wood. Meanwhile, the conversion efficiency of the TEG is assumed to be 2% and the recovery energy is around 10W. This gain is enough to feed low power devices such as phones, led lights and radios.

To achieve the maximum output power (P_{max}) of the TEG, the internal resistance should be equal to the load resistance i.e. R_{int}=R_L.

$$P_{max} = I_{TEG} * V_{TEG} \quad (12)$$

Depending on the required load power, the selection of the converter type is provided with MPPT to interface between the load and the TEG which helps consumers facilitate this technology in daily life with an economical approach.

TABLE III
VARIABLE ENERGY COST OF DIFFERENT ΔT

ΔT (°C)	Q_H (W)	P_{MPPT} (W)	η_{TEG}(%)	C_{TEG} ($/W)
80	58,76752	0,664	1,129876	9,036145
100	73,30646	0,986	1,345038	6,085193
130	96,09727	2,011	2,092671	2,98359

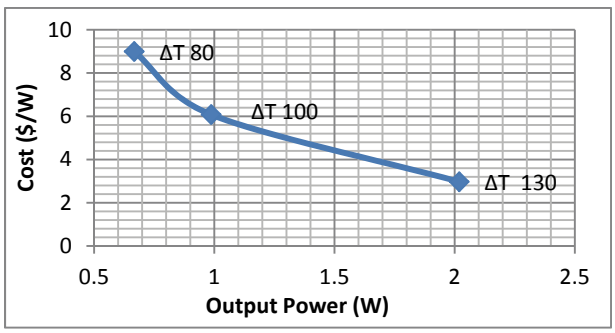

Fig. 19. Variable energy cost per watt.

VII. ECONOMIC PERSPECTIVE

Modern technology needs highly efficient devices with a low cost and the ability to convert waste heat into electric energy. This deficiency can be covered by manufacturing low-cost materials and well-automated mechanisms for TEG units. Additionally, the cost per watt of thermoelectric generator devices is aimed to be around 1 $/W for any installed system. To make this goal achievable, it is necessary to obtain a heat exchanger costs of $1/(W/K). Table III shows the variable operating cost per watt (C_{TEG}) for the proposed harvesting system which is calculated in Equ. (13).

$$C_{TEG}(\$/W) = \frac{\text{The Cost of Used TEG Units}}{P_{TEG\_MPPT}} \quad (13)$$

Fig. 19 illustrates the energy cost and the generated output power. It shows that the right selection of an operation temperature grantee a low cost and demonstrates the value of the SCP MPPT in grabbing the maximum power from a TEG system.

Several years ago, TEGs had limited development and were restricted to limited scenarios such as space and hard access zones. Some applications have a great significance but are still less requested by the market. Nowadays, TEGs are starting to be implemented in small or limited applications such as medical devices. On the other hand, most of the scientific research done in this field refers to the value of applying thermoelectric material in industry.

In terms of the TEG power production cost compared to photovoltaic cells, the TEG generates around 73 % of the power generated in photovoltaic cells. Meanwhile, the size and weight advantages are clearly held by the TEG [3]. Furthermore, the TEG can be implemented in a very flexible

way under different conditions. Meanwhile, the use of photovoltaic cells is very sensitive to surrounding conditions.

In the coming years, it is expected that the figure-of-merit of materials will reach an average of 2 and that this increase will reflect positively on power generation efficiency. Moreover, the primary concern for TEG product development and industrial viability is determining the appropriate fit between the product and potential commercial markets.

VIII. CONCLUSION

A high-performance SCP MPPT algorithm for TEG energy harvesting systems was implemented in this paper. The proposed algorithm used a new pulse technique to measure the short circuit current and to avoid disconnections between the load and the TEG array without measurements estimation. The SCP algorithm operates periodically based on the measurement of the short circuit current and accurately achieves the MPP according to the generated duty cycle. A simple and low-cost prototype was used to characterize the TEG array and to verify the operation point under different temperature gradients. Furthermore, the algorithm was applied under steady state and dynamic conditions with some advantages such as using a single current sensor and the use of a STM32F429 microcontroller, which allows the user to observe the measurements through its screen. Due to the small step of the duty cycle, the SCP algorithm operates successfully with small oscillations around the MPP. The proposed prototype is formalized experimentally and it presented the accurate performance.

REFERENCES

[1] D. Champier, "Thermoelectric generators: A review of applications," *Energy Conversion and Management*, Vol. 140, pp.167-181, May 2017.

[2] R. Kanan, "IoT devices: The quest for energy security," in *IEEE 59th International Midwest Symposium on Circuits and Systems,* pp. 1-4, 2016.

[3] O. M. Al-Habahbeh, A. Mohammad, A. Al-khalidi, M. Khanfer, and M. Obeid, "Design optimization of a large-scale thermoelectric generator," *Journal of King Saud University - Engineering Sciences*, Vol. 30, No. 2, pp. 177-182, Apr. 2018.

[4] W. Zhu, Y. Deng, Y. Wang, S. Shen, and R. Gulfam, "High-performance photovoltaic-thermoelectric hybrid power generation system with optimized thermal management," *Energy*, Vol. 100, pp. 91-101, Apr. 2016.

[5] H. Hashim, J. J. Bomphrey, and G. Min, "Model for geometry optimization of thermoelectric devices in a hybrid PV/TE system," *Renewable Energy*, Vol. 87, No. 1, pp. 458-463, Mar. 2016.

[6] A. Montecucco, A. R. Knox, and J. Siviter, "Combined heat and power system for stoves with thermoelectric generators," *Applied Energy*, Vol. 185, No. 2, pp. 1336-1342, Jan. 2017.

[7] G. J. Snyder, *Energy Harvesting Technologies*, Springer, Boston, MA, Chap. 11, pp. 325-336, 2009.

[8] L. Liu, "Feasibility of large-scale power plants based on thermoelectric effects," *New Journal of Physics*, Vol. 16, No. 12, pp.1-2, Dec. 2014.

[9] C. L. Izidoro, O. H. Ando Junior, J. P. Carmo, and L. Schaeffer, "Characterization of thermoelectric generator for energy harvesting," *Measurement*, Vol. 106, pp. 283-290, Aug. 2017.

[10] E. Sandoz-Rosado and R. J. Stevens, "Experimental Characterization of Thermoelectric Modules and Comparison with Theoretical Models for Power Generation," *J. Electron. Mater*, Vol. 38, No. 7, pp. 1239-1244, Jul. 2009.

[11] J. Vizquez, R. Palacios, M. A. Sanz-Bobi, and A. Arenas, "Test bench for measuring the electrical properties of commercial thermoelectric modules," in *Proc. Twenty-Second International Conference on-ICT*, pp. 589-593, 2003.

[12] R. Bonin, D. Boero, M. Chiaberge, and A. Tonoli, "Design and characterization of small thermoelectric generators for environmental monitoring devices," *Energy Conversion and Management*, Vol. 73, pp. 340-349, Sep. 2013.

[13] N. Phillip, O. Maganga, K. J. Burnham, M. A. Ellis, S. Robinson, J. Dunn, and C. Rouaud, "Investigation of maximum power point tracking for thermoelectric generators," *J. Electron. Mater.*, Vol. 42, No. 7, pp. 1900-1906, Jul. 2013.

[14] M. A. A. Faria, P. A. J. Stecanella, E. G. Domingues, P. H. G. Gomes, W. P. Calixto, and A. J. Alves, "Modeling, simulation and control of a thermoelectric generator," in Proc. *IEEE 15th International Conference on Environment and Electrical Engineering (EEEIC)*, Rome, pp. 1373-1378. 2015.

[15] L. X. Ni, K. Sun, L. Zhang, Y. Xing, M. Chen, and L. Rosendahl, "A power conditioning system for thermoelectric generator based on interleaved Boost converter with MPPT control," *2011 International Conference on Electrical Machines and Systems*, Beijing, pp. 1-6. 2011.

[16] E. A. Man, D. Sera, L. Mathe, E. Schaltz, and L. Rosendahl, "Thermoelectric generator emulator for MPPT testing," *2015 Intl Aegean Conference on Electrical Machines & Power Electronics (ACEMP), 2015 Intl Conference on Optimization of Electrical & Electronic Equipment (OPTIM) & 2015 Intl Symposium on Advanced Electromechanical Motion Systems (ELECTROMOTION)*, Side, pp. 774-778. 2015.

[17] S. Twaha, J. Zhu, Y. Yan, B. Li, and K. Huang, "Performance analysis of thermoelectric generator using DC-DC converter with incremental conductance based maximum power point tracking," *Energy for Sustainable Development*, Vol. 37, pp. 86-98, Apr. 2017.

[18] H. Yamada, K. Kimura, T. Hanamoto, T. Ishiyama, T. Sakaguchi, and T. Takahashi, "A MPPT control method of thermoelectric power generation with single sensor," *2013 IEEE 10th International Conference on Power Electronics and Drive Systems (PEDS)*, pp. 936-941. 2013.

[19] M. Bond and J. D. Park, "Current-sensorless power estimation and MPPT implementation for thermoelectric generators," *IEEE Trans. Ind. Electron.*, Vol. 62, No. 9, pp. 5539-5548, Sep. 2015.

[20] I. Laird, H. Lovatt, N. Savvides, D. Lu, and V. G. Agelidis, "Comparative study of maximum power point tracking algorithms for thermoelectric generators," *2008 Australasian Universities Power Engineering Conference*, pp. 1-6, 2008.
[21] A. Montecucco, Andrea, and A. R. Knox, "Maximum power point tracking converter based on the open-circuit voltage method for thermoelectric generators," *IEEE Trans. Power Electron.*, Vol. 30, No. 2, pp. 828-839, Feb. 2015.

Khalid Yahya received his B.S. degree in Electrical and Electronics Engineering from the University of Zawiya, Zawiya, Libya, in 2009; and his M.S. degree in Electrical Engineering from the Tun Hussein Onn University of Malaysia (UTHM), Batu Pahat, Malaysia. He is presently working towards his Ph.D. degree in Electrical Engineering at Kocaeli University, Kocaeli, Turkey. His current research interests include microelectronic circuit analysis and design, renewable energy resources, and power electronics and MPPT designs for energy harvesting systems.

Mehmet Zeki Bilgin received his Ph.D. degree in Electrical Engineering from Kocaeli University, Kocaeli, Turkey, in 2001. He is presently working as an Assistant Professor of Electrical Engineering at Kocaeli University, where he supervises the Power Electronics and Control Lab. His current research interests include energy harvesting systems for low power applications, renewable energy resources, electric vehicles, the control of electric machines and power converters.

Tarik Erfidan received his Ph.D. degree in Electrical Engineering from Kocaeli University, Kocaeli, Turkey, in 2004. He is presently working as an Assistant Professor of Electrical Engineering at Kocaeli University, where he supervises the Programmable Embedded Systems Lab and is the Head of the Microelectronics Device Reliability Program. His current research interests include microelectronics reliability, dc-dc converters in power electronics and renewable energy.